

# Additive Decomposition of the Physical Components of the Magnetic Coupling from Broken Symmetry Density Functional Theory Calculations

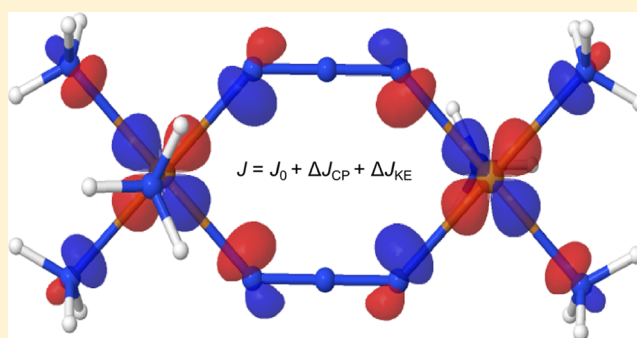
Esther Coulaud,<sup>†</sup> Jean-Paul Malrieu,<sup>‡</sup> Nathalie Guihéry,<sup>\*,‡</sup> and Nicolas Ferré<sup>\*,†</sup>

<sup>†</sup>Aix-Marseille Université, CNRS, Institut de Chimie Radicale, 13397, Marseille Cedex 20, France

<sup>‡</sup>Laboratoire de Chimie et Physique Quantiques, UMR 5626 of CNRS, Université de Toulouse III, 118 route de Narbonne, 31062 Toulouse, France

## S Supporting Information

**ABSTRACT:** The procedure to extract and identify from broken-symmetry density functional theory (BS-DFT) calculations the various components of the magnetic couplings in diradicals [*J. Chem. Phys.* **2012**, *137*, 114106] is re-examined. It is shown that this previous decomposition scheme fails for systems exhibiting large core polarization effects and hence becomes not additive in such cases. At variance, the new scheme which differs from the previous one in the assessment of the polarization effects is perfectly additive. As done previously, the direct exchange is calculated from the  $M_S = 1$  and  $M_S = 0$  restricted solutions. We show that allowing first the delocalization of the magnetic orbitals in the field of the closed shell frozen core furnishes a good evaluation of the kinetic exchange contribution to the magnetic exchange coupling, i.e. the intersite delocalization of the magnetic electrons in the low-spin state. In a second step, allowing the polarization of the core to take place in the field of the so-revised magnetic orbitals practically leads to the same total value of the magnetic coupling obtained by the brute-force BS-DFT calculation. The success of this decomposition is illustrated on a representative series of inorganic and organic diradicals. The obtained quasi-additivity of the effects is rationalized thanks to a careful theoretical analysis of the broken-symmetry solutions.



## 1. INTRODUCTION

The broken-symmetry (BS) approach, when used in the framework of the density functional theory (DFT), definitively appears as a privileged tool for the evaluation of magnetic couplings  $J$  in radicals and polyradicals. The performances of this BS-DFT approach have been well documented in several review papers.<sup>1–5</sup> Its main advantage relies on its simplicity and applicability to large systems, including the capability to optimize the geometries for high-spin states or lower  $M_S$  BS states and to extract subtle interactions such as the biquadratic exchange in systems of spin  $s = 1$ <sup>6</sup> or the double exchange interactions.<sup>7</sup> However, two main drawbacks have been acknowledged, namely the strong dependence of  $J$  to the choice of the exchange-correlation potential (which sometimes has to be tuned in order to reproduce experimental or high-level calculation values)<sup>1,8–10</sup> and the spin-contamination problem of the  $M_S = 0$  broken-symmetry solution which may be overcome according to various approximative treatments.<sup>11,12</sup> Recently, several approaches have been proposed to optimize the geometries of the spin decontaminated low-spin state.<sup>13–16</sup>

When affordable and provided that dynamic correlation is correctly taken into account (which may be very computation-

ally demanding), wave function-based ab initio methods are able to reach a very good accuracy and make eventually possible the decomposition of  $J$  in its various physical contributions.<sup>17,18</sup> The three main components are (a) the ferromagnetic direct exchange between the magnetic orbitals, (b) the antiferromagnetic kinetic exchange (or superexchange) provided by the intersite delocalization of the magnetic electrons, (c) the polarization of the nonmagnetic electrons. Albeit the latter mechanism is generally called spin-polarization, hereafter it will be more generally denoted core-polarization for reasons discussed in section 4.

With the idea to merge this decomposition procedure with BS-DFT calculations, we recently proposed a new approach based on the selective freezing of different classes of orbitals.<sup>19</sup> This idea of freezing some orbitals has already been used to decompose any interaction energy into its main electrostatic components, as proposed by Morokuma,<sup>20,21</sup> Ziegler,<sup>22</sup> Bagus,<sup>23</sup> or more recently Su,<sup>24</sup> or to constrain localized bond orbitals in QM/MM calculations.<sup>25</sup> Applied to ferromagnetic and antiferromagnetic systems featuring a

Received: April 15, 2013

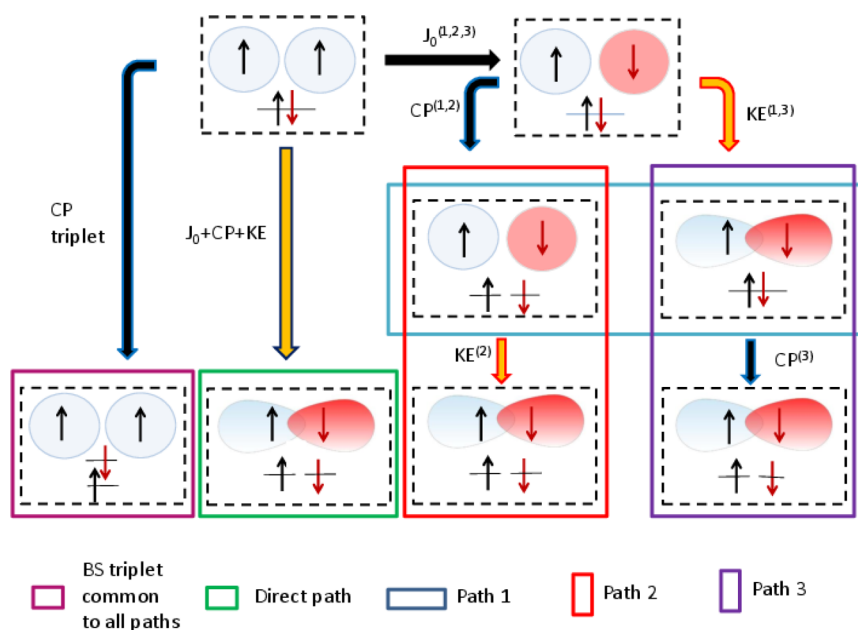


**Figure 1.** Illustrative representation of the three decomposition paths (first one in the blue box, second one in the red box, third in the purple box) and of the direct path (green box). One should pay attention to the fact that a similar picture is used for the various BS  $M_S = 0$  solutions despite their differences. The polarization of the core electrons results in a spatial displacement toward the magnetic site of the same spin.

moderate core-polarization contribution, the proposed strategy led to a reliable decomposition, i.e. the sum of the identified contributions quantitatively agreed with the total BS-DFT  $J$  value. However, its application to antiferromagnetic systems with a large core-polarizability (like azido bridges in binuclear copper systems) leads to a significantly poorer agreement, likely due to possible interferences between the delocalization and polarization mechanisms. Notice that this initial decomposition scheme showed almost no dependency to the choice of a DFT functional, as long as it includes a noticeable amount of Hartree–Fock exchange.<sup>19</sup>

In the present work, we first present two alternative decomposition schemes. As reported in section 2, we actually play with the relative order in which the magnetic orbital delocalization and the core orbital polarization are introduced. In section 3, the efficiency of the previously proposed and the new decomposition schemes are tested on a representative set of inorganic and organic diradicals with two 1/2-spins. In all cases, one of the new decomposition paths significantly improves the final value of  $J$  obtained as a sum of its various contributions. The reason for such a successful achievement is theoretically analyzed and discussed in section 4. Accordingly, a unique decomposition scheme is proposed for all the future applications.

## 2. THEORY: POSSIBLE DECOMPOSITION PATHS

Limiting the discussion to the case of two magnetic centers carrying spin  $S_i$  and  $S_j$ , the magnetic coupling is given as the effective interaction of the Heisenberg–Dirac–van Vleck Hamiltonian:

$$\mathcal{H} = -J\mathbf{S}_i \cdot \mathbf{S}_j \quad (1)$$

In the framework of BS-DFT, an estimate of the magnetic coupling is given by

$$J_{\text{UKS}} = -2\gamma(E_{\text{T,U}} - E_{\text{BS,U}}) \quad (2)$$

where  $\gamma$  introduces an ad-hoc correction of the spin-contaminated energies  $E_{\text{T,U}}$  and  $E_{\text{BS,U}}$ . In the following, we will adopt Yamaguchi's procedure<sup>11</sup> based on the mean values of  $S^2$ :

$$\gamma = \frac{1}{\langle S^2 \rangle_{\text{T}} - \langle S^2 \rangle_{\text{BS}}} \quad (3)$$

The three decomposition schemes are illustrated in Figure 1.

All the decomposition schemes start with a restricted open-shell DFT (RODFT) of the highest  $M_S$  component of the highest spin state, e.g.  $M_S = 1$  for a triplet state. Note this is always an eigenfunction of  $S^2$  with eigenvalue 2. The resulting singly occupied orbitals are then localized, defining two orthogonal magnetic orbitals  $a$  and  $b$ . This localization process is particularly easy in the case of centrosymmetric systems since it reduces to a  $\pi/4$  rotation of the symmetry-adapted  $g$  and  $u$  singly occupied molecular orbitals (MOs):

$$\begin{aligned} a &= \frac{1}{\sqrt{2}}(g + u) \\ b &= \frac{1}{\sqrt{2}}(g - u) \end{aligned} \quad (4)$$

The triplet function is  $\Phi_{\text{T,RO}} = |\Pi_i \bar{i} a b| = |\Pi_i \bar{i} g u|$  where  $i$  are the doubly occupied core MOs and its energy is  $E_{\text{T,RO}}$ . In the following, the product of core orbitals will be simply denoted  $\text{core}_{\text{T}}$  and  $\text{core}_{\text{BS}}$  for  $M_S = 1$  and  $M_S = 0$  solutions, respectively.

Using these magnetic orbitals and freezing all the core ones, one may calculate the energy  $E_{\text{BS,RO}}$  of the broken-symmetry determinant  $\Phi_{\text{BS,RO}} = |\text{core}_{\text{BS}} a b|$ :

$$E_{\text{BS,RO}} = E_{\text{T,RO}} + K_{ab} \quad (5)$$

where  $K_{ab}$  is related to the direct exchange between  $a$  and  $b$  orbitals through the selection of a suitable exchange–correlation functional. As it is explained in our previous work,<sup>19</sup> the direct exchange contribution to  $J$  is calculated as the energy difference

between  $\Phi_{T,RO}$  and a pure singlet state built from these orbitals, i.e.  $(1/\sqrt{2})(|core_{BS} \cdot a\bar{b}| + |core_{BS} \cdot b\bar{a}|)$ :

$$J_0 = 2K_{ab} \quad (6)$$

**First Decomposition Scheme.<sup>19</sup>** This proceeds through two independent relaxations of the orbitals.

1. Freezing the magnetic orbitals, the core ones are relaxed independently to minimize the energy of both the following  $M_S = 1$  triplet and  $M_S = 0$  broken-symmetry solutions:

$$\Phi_{T,UFM}^{(1)} = |core'_T \cdot a\bar{b}| \quad (7)$$

$$\Phi_{BS,UFM}^{(1)} = |core'_{BS} \cdot a\bar{b}| \quad (8)$$

where UFM means unrestricted formalism using frozen magnetic orbitals. The core-polarization contribution to  $J$  can be determined from the difference between the energies  $E_{T,UFM}^{(1)}$  and  $E_{BS,UFM}^{(1)}$  of the two solutions:

$$\Delta J_{CP}^{(1)} = -2\gamma(E_{T,UFM}^{(1)} - E_{BS,UFM}^{(1)}) - J_0 \quad (9)$$

In this particular case, the Coulomb fields felt by the  $\alpha$  and  $\beta$  core electrons are identical. Accordingly, the core-polarization contribution reduces to a spin-polarization process.

2. Freezing the core orbitals, the magnetic ones are relaxed to minimize the energy of the following  $M_S = 0$  broken-symmetry solution:

$$\Phi_{BS,UFC}^{(1)} = |core'_T \cdot a'\bar{b}'| \quad (10)$$

where UFC means unrestricted formalism using frozen core orbitals. This process allows each magnetic orbital to take a tail on the other center, introducing delocalization effects. With respect to our previous study, the constraint introduced by freezing the virtual orbitals in this relaxation process has been released to let  $a$  and  $\bar{b}$  interact with all the virtual orbitals. The corresponding additional energy gain is negligible and affects the kinetic exchange contribution of the studied compound at most by 4%. This shows that the main relaxation effect is brought by the partial delocalization of the magnetic orbitals on the other center:

$$a' = a\cos\theta + b\sin\theta; \quad b' = b\cos\theta + a\sin\theta \quad (11)$$

The kinetic exchange contribution to  $J$  can be determined from the difference between the energies  $E_{T,RO}$  and  $E_{BS,UFC}^{(1)}$ :

$$\Delta J_{KE}^{(1)} = -2\gamma(E_{T,RO} - E_{BS,UFC}^{(1)}) - J_0 \quad (12)$$

The total decomposition in scheme 1 finally reads as follows:

$$J^{(1)} = J_0 + \Delta J_{SP}^{(1)} + \Delta J_{KE}^{(1)} \quad (13)$$

This estimated magnetic coupling  $J^{(1)}$  has to be compared to  $J_{UKS}$  (eq 2).

**New Decomposition Scheme (Path 2).** This scheme proceeds first with the same core orbital relaxation as in scheme 1, giving access to the same  $\Delta J_{CP}^{(2)} = \Delta J_{CP}^{(1)}$  contribution. Accordingly, the core-polarization includes only spin-polarization. Then the magnetic orbitals are relaxed in the field of the spin-polarized core:

$$\Phi_{T,UFC}^{(2)} \simeq \Phi_{T,UFM}^{(1)} \quad (14)$$

$$\Phi_{BS,UFC}^{(2)} = |core'_{BS} \cdot a''\bar{b}''| \quad (15)$$

Attention must be paid to the fact that the frozen core here has already been spin-polarized in the previous step. As expected, the relaxation of the magnetic orbitals in the high-spin solution happens to be negligible. Then a modified evaluation of the kinetic exchange contribution is given by

$$\Delta J_{KE}^{(2)} = -2\gamma(E_{T,UFM}^{(1)} - E_{BS,UFC}^{(2)}) - J_0 \quad (16)$$

and a new total decomposition of the magnetic exchange is

$$J^{(2)} = J_0 + \Delta J_{CP}^{(2)} + \Delta J_{KE}^{(2)} \quad (17)$$

**New Decomposition Scheme (Path 3).** The third scheme proceeds first with the same magnetic orbital relaxation as in the original decomposition path, giving access to the same  $\Delta J_{KE}^{(3)} = \Delta J_{KE}^{(1)}$  contribution. Then the core orbitals are relaxed in the field of the magnetic orbitals  $a$  and  $b$  for the triplet and in the field of the relaxed (i.e., partially delocalized) magnetic orbitals  $a'$  and  $b'$  for the BS solution:

$$\Phi_{T,UFM}^{(3)} = \Phi_{T,UFM}^{(1)} \quad (18)$$

$$\Phi_{BS,UFM}^{(3)} = |core''_{BS} \cdot a'\bar{b}'| \quad (19)$$

It is noteworthy that in the  $M_S = 0$  solution, the  $\alpha$  and  $\beta$  core electrons now experience different Coulomb and spin fields. Accordingly, a modified evaluation of the core-polarization contribution is given by

$$\Delta J_{CP}^{(3)} = -2\gamma(E_{T,UFM}^{(3)} - E_{BS,UFC}^{(3)}) - J_0 \quad (20)$$

As will be discussed in section 4, this contribution is no longer a pure spin-polarization in this process since the coulomb field create by the magnetic electrons on the core electrons is no longer the same after the intersite delocalization of the magnetic orbitals. Accordingly the new total decomposition of the magnetic exchange reads

$$J^{(3)} = J_0 + \Delta J_{CP}^{(3)} + \Delta J_{KE}^{(3)} \quad (21)$$

### 3. COMPUTATIONAL INFORMATION

As illustrated in our previous paper,<sup>19</sup> the kinetic exchange contribution is negligible in ferromagnetic systems. For this reason, all the systems studied in this work are antiferromagnetic. For comparison purpose with the original decomposition scheme, we have first selected the binuclear complex  $Cu_2Cl_6^{2-}$  (denoted **1** in the following) in which two chlorine anions are bridging the two copper centers. Its geometry, corresponding to the crystal structure, is completely planar.<sup>18</sup> In this conformation, it shows a weak to moderate antiferromagnetic character. Following our previous study, its magnetic coupling interaction is computed using a modified B3LYP functional featuring 30% of Hartree–Fock exchange (instead of the original 20%) and the 6-31G(d,p) basis set.

At variance with this first example, the other three selected systems are expected to present important core-polarization contributions. The first one (denoted **2**) still belongs to the family of extensively studied (both experimentally and theoretically) inorganic systems: it features two Cu(II) centers bridged by  $N_3$  azido moieties and includes six coordinated amine  $NH_3$  ligands. Its crystal structure has been used to extract the coordinates of the cluster.<sup>18</sup> The selected level of theory is identical to **1**.

Next, we have selected the organic compound **3** as a typical  $\sigma$ -diradical. The *para*-benzynes  $C_6H_4$  is strongly antiferromag-

netic and its geometry in its singlet ground state has been recently optimized using the recently published spin-decontamination procedure coupled to BS-DFT calculations<sup>14</sup> and later validated by a less approximate approach.<sup>15</sup> Consistently, its  $J$  value is determined at the B3LYP/6-311G(d,p) level of theory.

Finally, the organic diradical **4** in which a phenylene bridge couples two nitroxide moieties features two  $\pi$  single electrons. This model system has been extensively studied by various ab initio and DFT methods. The CASPT2 geometry obtained by Calzado and co-workers<sup>26</sup> is used in the present work, while its  $J$  value is estimated and decomposed at the B3LYP/6-311G(d,p) level of theory.

Selective freezing of orbitals has been performed thanks to the local self-consistent-field method (LSCF)<sup>27</sup> as it is implemented in a locally modified version of the Gaussian package.<sup>28</sup>

Structures and magnetic orbital drawings have been made using Jmol<sup>29</sup> and are reported in Figure 2.

## 4. RESULTS AND DISCUSSION

**4.1. Analysis of the Results.** All the contributions to  $J$  arising from the application of the three decomposition schemes are reported in Tables 1–4. The absolute energies,

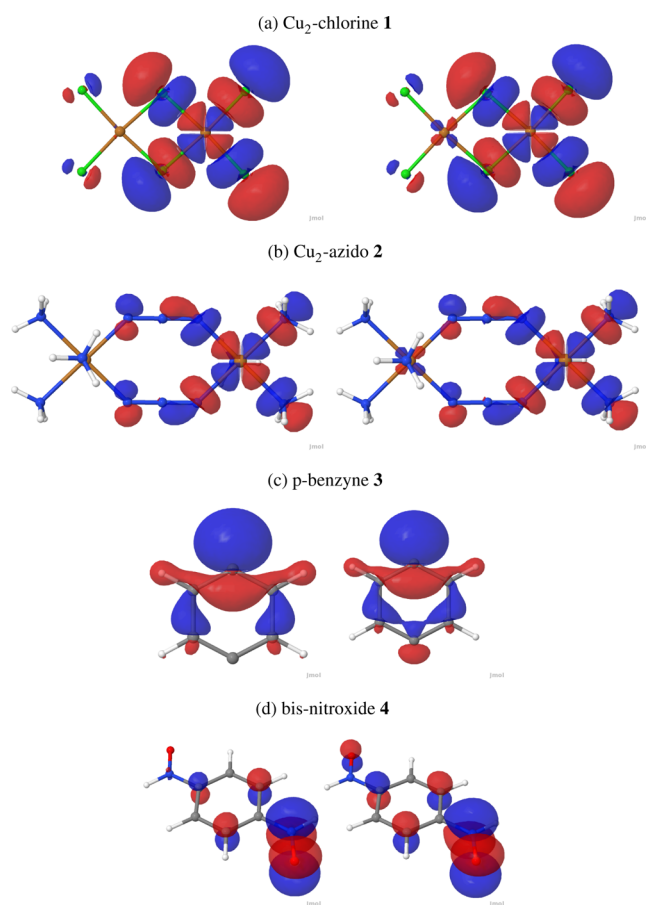


**Figure 2.** Structures and magnetic orbitals for compounds **1**–**4**. (left column) RODFT localized orbital (only one is shown, the other own is completely symmetric thanks to the molecular inversion center). (right column) Corresponding delocalized orbital obtained by the kinetic exchange mechanism.

the corresponding  $\langle S^2 \rangle$  values, and the geometries of the four compounds are given in the Supporting Information.

**Table 1.** Contributions in **1** ( $\text{cm}^{-1}$ )<sup>a</sup>

scheme $i$	1	2	3
$J_0$	107.0	107.0	107.0
$\Delta J_{\text{CP}}^{(i)}$	10.7	10.7	12.9
$\Delta J_{\text{KE}}^{(i)}$	(−140.1)	−115.5	−140.6
$(\Delta J_{\text{KE},ab}^{(i)})$	−140.6		
$J^{(i)}$	−22.9	2.3	−20.7
$J_{\text{UKS}}$			−21.3

<sup>a</sup>The best result  $J^{(i)}$  is highlighted in bold.

Compound **1** is weakly antiferromagnetic. As it can be seen in Table 1, the original decomposition scheme pointed out the small contribution to  $J$  due to the core-polarization mechanism ( $\Delta J_{\text{CP}}^{(1)} = 10.7 \text{ cm}^{-1}$ ), 1 order of magnitude less intense than the other two contributions and consistent with the absence of empty valence virtual orbitals in  $\text{Cl}^-$ . As mentioned in section 2, the kinetic exchange contribution can be more rigorously evaluated by allowing only the magnetic orbitals (one occupied, one virtual in each spin) to mix. The resulting  $\Delta J_{\text{KE},ab}^{(1)}$  value is only  $0.5 \text{ cm}^{-1}$  off the one obtained by using all the virtual orbitals to mix with the magnetic ones. Accordingly the kinetic exchange mechanism can be simply regarded as a delocalization process in a space spanned by two localized orbitals, as it is illustrated in Figure 2a.

In the second scheme, the decomposition starts with the core-polarization contribution, hence  $\Delta J_{\text{CP}}^{(1)} = \Delta J_{\text{CP}}^{(2)}$ . Then the magnetic orbitals are relaxed in the field of the polarized core orbitals, resulting in a kinetic exchange contribution which is different from the one obtained in the first decomposition scheme. Actually, its intensity is reduced by 18%. The consequence of such a reduction of  $\Delta J_{\text{KE}}$  is dramatically illustrated by the total magnetic exchange value,  $J^{(2)} = 2.3 \text{ cm}^{-1}$ , which appears to be ferromagnetic! The reduced antiferromagnetic kinetic exchange contribution cannot overtake the other contributions, all ferromagnetic.

In the third decomposition scheme, while the kinetic contribution is kept ( $\Delta J_{\text{KE}}^{(1)} = \Delta J_{\text{KE}}^{(3)} = -140.6 \text{ cm}^{-1}$ ), the core-polarization contribution is slightly modified:  $12.9 \text{ cm}^{-1}$  instead of  $10.7 \text{ cm}^{-1}$  obtained in the first two schemes. The resulting  $J^{(3)}$  differs only by  $-0.6 \text{ cm}^{-1}$  from the total value obtained using the standard BS-DFT approach.

The analysis concerning the magnetic exchange in compound **2** is completely different (Table 2). Using the decomposition scheme 1, both core-polarization and kinetic exchange contributions are antiferromagnetic. However, their sum is not large enough to allow  $J^{(1)}$  to be even in qualitative agreement with  $J_{\text{UKS}}$  (they differ by 14%). Compared with

**Table 2.** Contributions in **2** ( $\text{cm}^{-1}$ )<sup>a</sup>

scheme $i$	1	2	3
$J_0$	190.7	190.7	190.7
$\Delta J_{\text{CP}}^{(i)}$	−164.1	−164.1	−312.4
$\Delta J_{\text{KE}}^{(i)}$	−1222.3	−1196.4	−1222.3
$(\Delta J_{\text{KE},ab}^{(i)})$	(−1171.5)		
$J^{(i)}$	−1195.8	−1169.9	−1344.0
$J_{\text{UKS}}$			−1388.8

<sup>a</sup>The best result  $J^{(i)}$  is highlighted in bold.



compound **1**, the polarizable nature of the N<sub>3</sub> bridges is revealed by the significant  $\Delta J_{\text{CP}}^{(1)} = -164.1 \text{ cm}^{-1}$  contribution. Using the decomposition scheme 2, the kinetic exchange contribution is only slightly reduced. In other words, the mix of the magnetic orbitals (Figure 2b) is barely affected by the polarization of the core orbitals. As a result,  $J^{(2)}$  does not significantly differ from  $J^{(1)}$ . Notice that the kinetic exchange contribution is mainly due to the interactions of the magnetic orbitals with their virtual counterparts, as it was shown in compound **1**.

At variance with the previous situation, the core-polarization mechanism is enhanced by a factor of 2 when it operates on the relaxed magnetic orbitals, as it can be seen in scheme 3:  $\Delta J_{\text{CP}}^{(3)} = -312.4 \text{ cm}^{-1}$ . This larger contribution is enough to reach a better agreement with  $J_{\text{UKS}}$ , from which  $J^{(3)}$  differs only by  $-45 \text{ cm}^{-1}$  representing only 3% of the total  $J_{\text{UKS}}$  value.

In the case of compound **3** (Table 3), whatever the scheme, the core-polarization contribution is always antiferromagnetic.

**Table 3. Contributions in 3 (cm<sup>-1</sup>)<sup>a</sup>**

scheme <i>i</i>	1	2	3
$J_0$	353.0	353.0	353.0
$\Delta J_{\text{CP}}^{(i)}$	-287.9	-287.9	-275.6
$\Delta J_{\text{KE}}^{(i)}$	-2769.1	-2639.9	-2769.1
$(\Delta J_{\text{KE,ab}}^{(i)})$	(-2749.0)		
$J^{(i)}$	-2703.9	-2574.7	<b>-2691.6</b>
$J_{\text{UKS}}$			-2694.4

<sup>a</sup>The best result  $J^{(i)}$  is highlighted in bold.

Nevertheless it cannot overcome the direct exchange contribution. Moreover, contrary to compounds **1** and **2**, its intensity is reduced when obtained in the presence of the relaxed magnetic orbitals ( $-275.6$  vs  $-287.9 \text{ cm}^{-1}$ ). The latters are represented in Figure 2c. The kinetic exchange contribution is largely reduced by the polarization of the core orbitals. Consequently,  $J^{(2)}$  shows the worst agreement with  $J_{\text{UKS}}$ : they differ by  $65 \text{ cm}^{-1}$ . Here again, the best decomposition is obtained by application of scheme 3,  $J^{(3)}$  being virtually equal to  $J_{\text{UKS}}$ . Finally note that  $\Delta J_{\text{KE,ab}}^{(1)}$  differs only by  $-20 \text{ cm}^{-1}$  from  $\Delta J_{\text{KE}}^{(1)}$ , in agreement with the observations made in compounds **1** and **2**.

Finally, the analysis of  $J$  contributions in compound **4** (Table 4) qualitatively follow the one we made in the case of

**Table 4. Contributions in 4 (cm<sup>-1</sup>)<sup>a</sup>**

scheme <i>i</i>	1	2	3
$J_0$	239.0	239.0	239.0
$\Delta J_{\text{CP}}^{(i)}$	-572.0	-572.0	-640.7
$\Delta J_{\text{KE}}^{(i)}$	-3243.7	-3097.8	-3243.7
$(\Delta J_{\text{KE,ab}}^{(i)})$	(unconverged)		
$J^{(i)}$	-2703.9	-3430.8	<b>-3645.4</b>
$J_{\text{UKS}}$	-3576.7		-3664.6

<sup>a</sup>The best result  $J^{(i)}$  is highlighted in bold.

compound **2**. The core-polarization contribution is enhanced when determined after having relaxed the magnetic orbitals (Figure 2d), while the kinetic exchange contribution is reduced when calculated in the field of the polarized core orbitals. Here again,  $J^{(2)}$  gives the worst agreement with  $J_{\text{UKS}}$  and  $J^{(3)}$  only differs from it by less than  $20 \text{ cm}^{-1}$ , definitively confirming the

superiority of the decomposition scheme 3 over the two other ones.

From all the results presented above, it is clear that the decomposition scheme 3, corresponding to path 3 in Figure 1, gives the best agreement with full BS-DFT calculations. Accordingly, we strongly suggest to use this approach in any future application. Moreover, it is also possible to calculate the  $t$  and  $U$  parameters of a Hubbard model Hamiltonian, from the expectation values of  $S^2$  in the  $M_S = 0$  broken symmetry solution and the energies of the various solutions. This Hamiltonian, when restricted to the two magnetic electrons in their magnetic orbitals, leads to a  $2 \times 2$  configuration interaction matrix between the neutral valence bond component of energy zero and the ionic component, of energy  $U$  (which is the on site coulomb repulsion). The coupling between these two VB components is  $2t$  where  $t$  is the intersite hopping integral.

The analytical expressions of these parameters are

$$t = \frac{E(\Phi_{\text{T,RO}}) - E(\Phi_{\text{BS,UFC}})}{\sqrt{1 - \langle S^2 \rangle}}$$

$$U = 2 \frac{E(\Phi_{\text{T,RO}}) - E(\Phi_{\text{BS,UFC}})}{1 - \langle S^2 \rangle} - J_0 \quad (22)$$

The kinetic exchange contribution can also be evaluated from these parameters using the expression:

$$\Delta J_{\text{KE}}^{U,t} = \frac{U - \sqrt{U^2 + 16t^2}}{2} \quad (23)$$

The corresponding values for the studied compounds **1–4** are reported in Table 5. One should note that the kinetic exchange

**Table 5. Hubbard  $t$  and  $U$  Parameters<sup>a</sup>**

compound	$ t $	$U$	$\Delta J_{\text{KE}}^{U,t}$
<b>1</b>	308	11160	-34
<b>2</b>	3501	46305	-1036
<b>3</b>	4171	25801	-2462
<b>4</b>	4402	22090	-3079

<sup>a</sup>Kinetic exchange contribution evaluated from eq 23 using decomposition path 3. All values are in inverse centimeters.

contribution calculated using this expression is free from spin contamination. On the contrary, the core relaxation of both the triplet  $M_S = 1$  and broken symmetry  $M_S = 0$  solutions introduces components of higher multiplicity states, i.e. essentially quintet for the triplet and triplet for the  $M_S = 0$  solution. A rigorous spin decontamination would be hard to perform.

It is noteworthy that the  $\Delta J_{\text{KE}}^{U,t}$  are in a good agreement with the values of  $\Delta J_{\text{KE}}$  obtained with decomposition path 3, validating a posteriori the use of this effective Hubbard Hamiltonian.

**4.2. Rationalization of the Superiority of Path 3.** The broken symmetry  $M_S = 0$  solution  $\Phi_{\text{BS,UFC}}$  is obtained using the  $a'$  and  $b'$  orbitals and contains ionic components which are pure singlets. Since the closed shell ionic components cannot spin-polarize the core electrons, the spin-polarization of the latter is expected to be smaller in the  $\Phi_{\text{BS,UFC}}^{(3)}$  than in the  $\Phi_{\text{BS,UFC}}^{(1)}$ , which only involves neutral components since it is obtained using the  $a$  and  $b$  MOs from the triplet state. As a

consequence, the spin-polarization is expected to be larger in path 1 and 2 than in path 3. Looking at the results obtained for compounds 2 and 4, the core relaxation brings a larger contribution to the magnetic exchange in path 3 than in path 1 and 2, suggesting that another contribution than the spin-polarization is involved in the core relaxation. On the basis of the simple Hartree–Fock approach, the present subsection analyses the possible origin of these other contributions. The following rationalization is based on the isomorphism between the Hartree–Fock and Kohn–Sham mean-field treatments.

The ROHF function for  $M_S = 1$   $\Phi_{\text{T,UFM}}^{(1)}$  satisfies the Brillouin's theorem, namely:

$$\langle (a_i^\dagger a_i + a_{i^*}^\dagger a_{i^*}) \Phi_{\text{T,UFM}}^{(1)} | \mathcal{H} | \Phi_{\text{T,UFM}}^{(1)} \rangle = 0 \quad (24)$$

$$\langle i^* | h^c + J_a + J_b - \frac{K_a}{2} - \frac{K_b}{2} | i \rangle = 0 \quad (25)$$

where  $h^c$  involves the kinetic, nuclear and the core electrons Fock field operators. For the triplet state, the polarization of the core electrons in the unrestricted formalism is a pure spin-polarization effect. The mixing between the  $i$  and  $i^*$  orbitals are opposite for the  $\alpha$  and  $\beta$  core spinorbitals:

$$\begin{aligned} \langle a_i^\dagger a_i \Phi_{\text{T,UFM}}^{(1)} | \mathcal{H} | \Phi_{\text{T,UFM}}^{(1)} \rangle \\ = - \langle a_{i^*}^\dagger a_{i^*} \Phi_{\text{T,UFM}}^{(1)} | \mathcal{H} | \Phi_{\text{T,UFM}}^{(1)} \rangle \\ = \langle i^* | -\frac{K_a}{2} - \frac{K_b}{2} | i \rangle \end{aligned} \quad (26)$$

This leads to the following spin-polarization contribution of the triplet state:

$$\Delta E_{\text{T,UFM}}^{\text{CP}} = 2 \sum_{i,i^*} \frac{\langle i | (K_a + K_b) / 2 | i^* \rangle^2}{\varepsilon_i - \varepsilon_{i^*}} \quad (27)$$

in which  $\varepsilon_i$  (respectively,  $\varepsilon_{i^*}$ ) denotes the energy of the occupied core (resp virtual) orbital  $i$  (resp  $i^*$ ). The spin-polarization contribution to the broken symmetry  $M_S = 0$  solution obtained using the triplet MOs is

$$\Delta E_{\text{BS,UFM}}^{\text{CP}} = 2 \sum_{i,i^*} \frac{\langle i | (K_a - K_b) / 2 | i^* \rangle^2}{\varepsilon_i - \varepsilon_{i^*}} \quad (28)$$

After the spin decontamination, which multiplies this contribution by a factor close to 2, this results in a spin-polarization contribution to  $J$  in the first and second decomposition paths close to the exact second-order correction:<sup>17</sup>

$$\Delta J_{\text{CP}}^{(1,2)} = 4 \sum_{i,i^*} \frac{\langle i^* | K_a | i \rangle \langle i | K_b | i^* \rangle}{\varepsilon_i - \varepsilon_{i^*}} \quad (29)$$

Let us now consider the solutions obtained using the relaxed  $a'$  and  $b'$  orbitals. The effect of the core orbital optimization in the field of the magnetic electrons is given by the second-order effect of the single  $i \rightarrow i^*$  excitations. The interaction between  $\Phi_{\text{BS,UFM}}$  and the singly excited determinants is now

$$\begin{aligned} \langle a_i^\dagger a_i \Phi_{\text{BS,UFM}} | \mathcal{H} | \Phi_{\text{BS,UFM}} \rangle &= \langle i^* | h^c + J_{a'} + J_{b'} - K_a | i \rangle \\ \langle a_{i^*}^\dagger a_{i^*} \Phi_{\text{BS,UFM}} | \mathcal{H} | \Phi_{\text{BS,UFM}} \rangle &= \langle i^* | h^c + J_{a'} + J_{b'} - K_b | i \rangle \end{aligned} \quad (30)$$

One may use a simple trick to further develop these expressions. Subtracting the ROHF Fock operator matrix element for the original (nonpolarized) orbitals  $i$  and  $i^*$ ,

$$\langle i^* | F | i \rangle = \left\langle i^* \left| h^c + J_a + J_b - \frac{K_a + K_b}{2} \right| i \right\rangle \quad (31)$$

and similarly  $\langle i^* | F | i \rangle$ , both of them being zero, the previous expressions read

$$\begin{aligned} \langle a_i^\dagger a_i \Phi_{\text{BS,UFM}} | \mathcal{H} | \Phi_{\text{BS,UFM}} \rangle \\ = \langle i^* | J_{a'} + J_{b'} - K_{a'} - J_a - J_b + \frac{K_a + K_b}{2} | i \rangle \\ \langle a_{i^*}^\dagger a_{i^*} \Phi_{\text{BS,UFM}} | \mathcal{H} | \Phi_{\text{BS,UFM}} \rangle \\ = \langle i^* | J_{a'} + J_{b'} - K_{b'} - J_a - J_b + \frac{K_a + K_b}{2} | i \rangle \end{aligned} \quad (32)$$

These integrals are easier to understand if we first analyze their exchange part, which is responsible for the spin-polarization:

$$\begin{aligned} \langle i^* | -K_{a'} + \frac{K_a + K_b}{2} | i \rangle \\ = \langle i^* | (-K_a + K_b)(\cos^2 \theta - 1/2) | i \rangle \\ + [(i^* a, ib) + (i^* b, ia)] \sin \theta \cos \theta \end{aligned} \quad (33)$$

having used the development of the two-electron exchange integral

$$\begin{aligned} \langle i^* | K_a | i \rangle &= (i^* a', ia') \\ &= (i^* [\cos \theta a + \sin \theta b], i [\cos \theta a + \sin \theta b]) \\ &= \cos^2 \theta \langle i^* | K_a | i \rangle + \sin^2 \theta \langle i^* | K_b | i \rangle \\ &\quad + \cos \theta \sin \theta [(i^* a, ib) + (i^* b, ia)] \end{aligned} \quad (34)$$

One may expect that the two last integrals are very small in many cases. The first term of the right member of the equation is similar to the interaction appearing when using the  $a$  and  $b$  orbitals except for the factor  $1/2$  which is now  $(\cos^2 \theta - 1/2)$ . The spin-polarization effect decreases proportionally to  $\theta^2$  for small mixings of the orbitals.

Now considering the effect of the Coulomb part appearing in this interaction (eq 32), namely the difference between the electric field created by the  $(a'b')$  distribution with respect to the one created by  $(ab)$ , one may express  $J_{a'} + J_{b'}$  as a function of the angle  $\theta$ . Using

$$\begin{aligned} a'a' &= aa \cos^2 \theta + bb \sin^2 \theta + 2ab \sin \theta \cos \theta \\ b'b' &= bb \cos^2 \theta + aa \sin^2 \theta + 2ab \sin \theta \cos \theta \end{aligned} \quad (35)$$

the Coulombic part of the interaction reads

$$\langle i^* | J_{a'} + J_{b'} - J_a - J_b | i \rangle = 2(ii^*, ab) \sin 2\theta \quad (36)$$

This integral represents the interaction between the transition dipoles associated to the  $ii^*$  and  $ab$  distributions. If the tails of the magnetic orbitals on the bridging ligands are large, this contribution will not be negligible and the orbital relaxation of the core orbitals in the field of the relaxed magnetic orbitals will present some electrostatic polarization content.

This effect may be responsible for the observed significative increase of the core relaxation energy in path 3 in compounds 2 and 4. In case of compound 3, the magnetic orbitals being of  $\sigma$

character, the integrals ( $ii^*,ab$ ) are expected to be small since the  $\pi$  and  $\pi^*$  orbitals, which are the most polarizable, have a nodal plane in the region of the  $\sigma$  magnetic orbitals.

As a final note, the modifications of the values of  $\langle S^2 \rangle$  have been analyzed along the three different decomposition paths (values reported in the Supporting Information). Two opposite effects can be highlighted. First, the intersite delocalization of the magnetic electrons, which introduces ionic components, always decreases  $\langle S^2 \rangle$ . Second, the core polarization (pure spin polarization in path 2 or spin + Coulomb polarization in path 3) increases this quantity, since it introduces 4-open-shell determinants in the basis of orthogonal MOs, which necessarily have quintet components. This remark shows the limits of the spin decontamination procedures, which are valid for the intersite delocalization of the magnetic electrons, but less relevant for the spin polarization effects. Finally we have noticed that the amplitudes of the variations of  $\langle S^2 \rangle$  are in line with the corresponding energy corrections: the larger the variation of  $\langle S^2 \rangle$  (in absolute value), the larger the energy contribution.

## 5. CONCLUSION

The understanding of the physical factors governing the magnitude of the magnetic coupling between unpaired electrons localized in different sites of a molecule or lattice is an important contribution of quantum chemistry to the theory of molecular magnetism. In this regard, one must quote the pioneer and deep contributions of Kahn to this understanding.<sup>30</sup> This understanding does not bring only an intellectual satisfaction. Playing with the various mechanisms entering in the couplings, it offers firm suggestions to conceive molecular or periodic lattices exhibiting the desired properties for instance ferro- or ferrimagnetic lattices.<sup>30,31</sup>

Wave function based methods may eventually afford an analysis of distinct mechanisms entering in the magnetic coupling.<sup>17,18,32</sup> Rooted in the DFT, the very convenient broken symmetry Kohn–Sham approach is a popular tool, despite the sensitivity of its results to the chosen exchange correlation functional. Until recently, it essentially furnishes a number for the magnetic exchange, without providing a decomposition of the magnetic exchange into various contributions. At variance with our previous work<sup>19</sup> which was not accurate enough for diradicals whose core polarization contributes significantly to  $J$ , the present paper introduces an almost additive decomposition scheme which enables one to distinguish unambiguously the contributions of direct exchange, kinetic exchange, and core polarization effects, and to evaluate their relative amplitudes. The method proceeds through a short series of partially relaxed/partially frozen DFT calculations.

The validity of the decomposition is tested by comparing the sum of the so-identified contributions to the direct evaluation of the magnetic coupling. The three decomposition paths have been tested on a set of copper  $d^9$  dimers, on a  $\sigma$ -diradical hydrocarbon and on a  $\pi$ -diradical bis-nitroxide. The decomposition path which starts with the magnetic orbital relaxation in the  $M_S = 0$  BS solution and then relaxes the core orbitals in the field of the new magnetic orbitals appears as the best one. Actually a deep theoretical analysis of BS solutions demonstrates that the core polarization in this process does not reduce to a spin-polarization, the Coulomb field created by the relaxed electronic distribution of the magnetic electrons being different from that created by the these electrons in the triplet state.

The procedure is simple and can easily be implemented in standard DFT codes for analyzing results obtained by more involved procedures.<sup>33–35</sup> From the computational point of view, we will also investigate more deeply how the choice of the DFT functional may affect the relative intensities of each contribution to the magnetic coupling.

Finally, the method may also be applied to magnetic systems either involving more than two spin  $s = 1/2$  or bearing spin momenta larger than  $1/2$ . In the case of three centers A, B, and C bearing a spin  $s = 1/2$ , the usual procedure consists in calculating the highest  $M_S = 3/2$  solution  $|\text{core}'\cdot a\cdot b\cdot c|$  and the three  $M_S = 1/2$  broken symmetry solutions in which either  $a$ ,  $b$ , or  $c$  orbital bears a down spin, from which  $J_{ab}$ ,  $J_{ac}$  and  $J_{bc}$  can be extracted. In the first step, the spin unrestricted determinants  $|\text{core}\cdot\bar{a}\cdot b\cdot c|$ ,  $|\text{core}\cdot a\cdot\bar{b}\cdot c|$ , and  $|\text{core}\cdot a\cdot b\cdot\bar{c}|$  are calculated using the orbitals of the (RODFT)  $M_S = 3/2$  solution, in order to determine the direct exchange values  $K_{ab}$ ,  $K_{bc}$ , and  $K_{ac}$ . Then freezing the core orbitals of the restricted high spin solution and relaxing the magnetic orbitals provides the kinetic contributions to the three magnetic couplings. Finally in a third step, the relaxation of the core orbitals allows the core polarization to take place. For systems of two magnetic centers of  $s = 1$  for instance, the usual procedure consists in calculating the highest ( $M_S = 2$ ) and lowest ( $M_S = 0$ ) spin unrestricted solutions. Again, the same three-step scheme can of course be applied to distinguish the direct exchange, the kinetic, and the core polarization contributions to the magnetic couplings.

In future applications, we will use this decomposition scheme to treat large diradical systems, allowing to estimate how inter- and intramolecular magnetic couplings may be affected by chemical substitutions at key positions surrounding the magnetic centers or by environmental effects like a solvent.<sup>36</sup> The procedure will also be applied to polyradicalar systems both organic and inorganic and to systems involving centers bearing high spin momentum.

## ■ ASSOCIATED CONTENT

### Supporting Information

Cartesian coordinates for compounds 1–4. Details of the decomposition analysis (absolute energies and  $\langle S^2 \rangle$ ). This material is available free of charge via the Internet at <http://pubs.acs.org/>.

## ■ AUTHOR INFORMATION

### Corresponding Author

\*E-mail: [nathalie.guihery@irsamc.ups-tlse.fr](mailto:nathalie.guihery@irsamc.ups-tlse.fr) (N.G.); [nicolas.ferre@univ-amu.fr](mailto:nicolas.ferre@univ-amu.fr) (N.F.).

### Notes

The authors declare no competing financial interest.

## ■ ACKNOWLEDGMENTS

All the computations have been performed at the “Centre Régional de Compétences en Modélisation Moléculaire” in Marseille, France.

## ■ REFERENCES

- (1) Illas, F.; de, P. R.; Moreira, I.; Bofill, J. M.; Filatov, M. *Phys. Rev. B* **2004**, *70*, 132414.
- (2) Bencini, A. *Inorg. Chim. Acta* **2008**, *361*, 3820–3831.
- (3) Cramer, C. J.; Truhlar, D. G. *Phys. Chem. Chem. Phys.* **2009**, *11*, 10757–10816.
- (4) Neese, F. *Coord. Chem. Rev.* **2009**, *253*, 526–563.
- (5) Swart, M. *Int. J. Quantum Chem.* **2013**, *113*, 2–7.

- (6) Labèguerie, P.; Boilleau, C.; Bastardis, R.; Suaud, N.; Guihéry, N.; Malrieu, J.-P. *J. Chem. Phys.* **2008**, *129*, 154110.
- (7) Boilleau, C.; Suaud, N.; Bastardis, R.; Guihéry, N.; Malrieu, J.-P. *Theor. Chem. Acc.* **2010**, *126*, 231.
- (8) Peralta, J. E.; Melo, J. I. *J. Chem. Theory Comput.* **2010**, *6*, 1894–1899.
- (9) Ruiz, E. *J. Comput. Chem.* **2011**, *32*, 1998–2004.
- (10) Phillips, J. J.; Peralta, J. E. *J. Chem. Theory Comput.* **2012**, *8*, 3147–3158.
- (11) Soda, T.; Kitagawa, Y.; Onishi, T.; Takano, Y.; Shigeta, Y.; Nagao, H.; Yoshioka, Y.; Yamaguchi, K. *Chem. Phys. Lett.* **2000**, *319*, 223–230.
- (12) Ciofini, I.; Daul, C. A. *Coord. Chem. Rev.* **2003**, *238–239*, 187–209.
- (13) Swart, M.; Güell, M.; Luis, J. M.; Solà, M. *J. Phys. Chem. A* **2010**, *114*, 7191–7197.
- (14) Malrieu, J.-P.; Trinquier, G. *J. Phys. Chem. A* **2012**, *116*, 8226–8237.
- (15) Saito, T.; Thiel, W. *J. Phys. Chem. A* **2012**, *116*, 10864–10869.
- (16) Hratchian, H. P. *J. Chem. Phys.* **2013**, *138*, 101101.
- (17) Calzado, C. J.; Cabrero, J.; Malrieu, J. P.; Caballol, R. *J. Chem. Phys.* **2002**, *116*, 2728–2747.
- (18) Calzado, C. J.; Angeli, C.; Taratiel, D.; Caballol, R.; Malrieu, J.-P. *J. Chem. Phys.* **2009**, *131*, 044327.
- (19) Coulaud, E.; Guihéry, N.; Malrieu, J.-P.; Hagebaum-Reignier, D.; Siri, D.; Ferré, N. *J. Chem. Phys.* **2012**, *137*, 114106.
- (20) Kitaura, K.; Morokuma, K. *Int. J. Quantum Chem.* **1976**, *10*, 325–340.
- (21) Uneyama, H.; Morokuma, K. *J. Am. Chem. Soc.* **1977**, *99*, 1316–1332.
- (22) Ziegler, T.; Rauk, A. *Inorg. Chem.* **1979**, *18*, 1558–1565.
- (23) Bagus, P. S.; Hermann, K.; Bauschlicher, C. W., Jr. *J. Chem. Phys.* **1984**, *80*, 4378–4386.
- (24) Su, P.; Li, H. *J. Chem. Phys.* **2009**, *131*, 014102.
- (25) Ferré, N.; Assfeld, X.; Rivail, J.-L. *J. Comput. Chem.* **2002**, *23*, 610–624.
- (26) Calzado, C. J.; Angeli, C.; de Graaf, C.; Caballol, R. *Theor. Chem. Acc.* **2011**, *128*, 505–519.
- (27) Assfeld, X.; Rivail, J.-L. *Chem. Phys. Lett.* **1996**, *263*, 100–106.
- (28) Frisch, M. J.; Trucks, G. W.; Schlegel, H. B.; Scuseria, G. E.; Robb, M. A.; Cheeseman, J. R.; Scalmani, G.; Barone, V.; Mennucci, B.; Petersson, G. A.; Nakatsuji, H.; Caricato, M.; Li, X.; Hratchian, H. P.; Izmaylov, A. F.; Bloino, J.; Zheng, G.; Sonnenberg, J. L.; Hada, M.; Ehara, M.; Toyota, K.; Fukuda, R.; Hasegawa, J.; Ishida, M.; Nakajima, T.; Honda, Y.; Kitao, O.; Nakai, H.; Vreven, T.; Montgomery, J. A., Jr.; Peralta, J. E.; Ogliaro, F.; Bearpark, M.; Heyd, J. J.; Brothers, E.; Kudin, K. N.; Staroverov, V. N.; Kobayashi, R.; Normand, J.; Raghavachari, K.; Rendell, A.; Burant, J. C.; Iyengar, S. S.; Tomasi, J.; Cossi, M.; Rega, N.; Millam, J. M.; Klene, M.; Knox, J. E.; Cross, J. B.; Bakken, V.; Adamo, C.; Jaramillo, J.; Gomperts, R.; Stratmann, R. E.; Yazyev, O.; Austin, A. J.; Cammi, R.; Pomelli, C.; Ochterski, J. W.; Martin, R. L.; Morokuma, K.; Zakrzewski, V. G.; Voth, G. A.; Salvador, P.; Dannenberg, J. J.; Dapprich, S.; Daniels, A. D.; Farkas, O.; Foresman, J. B.; Ortiz, J. V.; Cioslowski, J.; Fox, D. J. *Gaussian 09*, revision A.02; Gaussian Inc.: Wallingford CT, 2009.
- (29) <http://www.jmol.org>. (accessed April 14, 2013).
- (30) Kahn, O. *Molecular magnetism*; Wiley Online Library: New York, 1994; Vol. 25; pp 1–396.
- (31) Verdaguer, M. *Polyhedron* **2001**, *20*, 1115–1128.
- (32) Terencio, T.; Bastardis, R.; Suaud, N.; Maynau, D.; Bonvoisin, J.; Malrieu, J. P.; Calzado, C. J.; Guihéry, N. *Phys. Chem. Chem. Phys.* **2011**, *13*, 12314–12320.
- (33) Samanta, K.; Jiménez-Hoyos, C. A.; Scuseria, G. E. *J. Chem. Theory Comput.* **2012**, *8*, 4944–4949.
- (34) Barone, V.; Boilleau, C.; Cacelli, I.; Ferretti, A.; Monti, S.; Prampolini, G. *J. Chem. Theory Comput.* **2013**, *9*, 300–307.
- (35) Phillips, J. J.; Peralta, J. E. *J. Chem. Phys.* **2013**, *138*, 174115.
- (36) Coulaud, E.; Hagebaum-Reignier, D.; Siri, D.; Tordo, P.; Ferré, N. *Phys. Chem. Chem. Phys.* **2012**, *14*, 5504–5511.